Eur. Phys. J. A **19**, 83–87 (2004)
DOI 10.1140/epja/i2003-10105-4

THE EUROPEAN PHYSICAL JOURNAL A

Reinvestigation of the beta-decay of ^{110}Mo

J.C. Wang[a], P. Dendooven, S. Hankonen, J. Huikari, A. Jokinen, V.S. Kolhinen, G. Lhersonneau, A. Nieminen, K. Peräjärvi, S. Rinta-Antila, and J. Äystö

Department of Physics, University of Jyväskylä, FIN-40351 Jyväskylä, Finland

Received: 5 May 2003 / Revised version: 13 June 2003 /
Published online: 26 November 2003 –
Communicated by D. Guerreau

Abstract. The beta-decay of the neutron-rich nucleus ^{110}Mo, separated by the IGISOL on-line mass separator from other fission products, has been investigated by using beta-gamma and gamma-gamma coincidence techniques. The decay scheme of ^{110}Mo has been revised, including 3 new excited states and 7 new γ transitions in ^{110}Tc. The β-feedings were measured and $\log ft$ values and B(GT) values were deduced based on a Q_β-value from systematics. Three excited 1^+ states in ^{110}Tc fed by spin-flip allowed-unhindered beta transitions were identified. The deduced beta-decay strengths are compared with the Gamow-Teller strength distribution obtained from a macroscopic-microscopic calculation. The role of the asymptotic quantum numbers in the context of the allowed beta-decay is discussed.

PACS. 27.60.+j $90 \leq A \leq 149$ – 21.10.Tg Lifetimes – 23.20.Lv Gamma transitions and level energies

1 Introduction

Studies of the β^--decay of exotic nuclei far from the line of stability provide an important contribution to understanding the weak-interaction mechanism and nuclear-structure features of neutron-rich nuclei. It also provides the basic information for studies of heavy-element synthesis in stellar environments and double beta-decay.

In the neutron-rich mass region between the nearly spherical $Z = 50$ (Sn) and the strongly deformed $Z = 40$ (Zr) nuclei, fast allowed beta-decay to low-lying states is expected to occur between the spin-orbit partner shell model orbits $g_{7/2}$ and $g_{9/2}$. In the spherical shell model only one $0^+ \rightarrow 1^+$ Gamow-Teller (GT) transition is expected corresponding to the transformation of a $g_{7/2}$ neutron into a $g_{9/2}$ proton. When nuclei are deformed, spherical single-particle states are split into Nilsson states which can be described by the asymptotic quantum numbers $\Omega^\pi[\mathrm{Nn}_z\Lambda\Sigma]$ [1]. In this case, beta-decay will obey the additional asymptotic quantum number selection rules. If $\Delta\Omega = 1$, $\Delta N = \Delta n_z = \Delta\Lambda = 0$, the beta transition is called allowed-unhindered (au) [2]. Such kind of transitions can be identified by their low $\log ft$ values ($\log ft \leqslant 5$). If $\Delta\Omega = 1$, $\Delta N = \Delta n_z = \Delta\Lambda = 0$ or 1, the beta-decay is called allowed-fast which is relatively fast, though slower than the au transitions [3]. All other allowed transitions violating the asymptotic quantum number selection rules are called allowed-hindered.

Systematics of au transitions have been evaluated in great detail in the rare-earth region [4], where they connect states originating from the $h_{9/2}$ and $h_{11/2}$ unique-parity orbits across the major shell. The beta-decays of the even-even $^{114-120}$Pd, $^{110-114}$Ru and $^{102-108}$Mo nuclei were studied using the ion guide isotope separator IGISOL in Jyväskylä [5–9]. In these nuclei, the GT strength was found to reside mainly in two to four $0^+ \rightarrow 1^+$ transitions with their $\log ft$ values between 4.4 and 5.1. These observations are in agreement with the deformed-shell-model predictions in which the sequence of Nilsson states implies four candidates for au pairs in this region, namely $\nu 7/2[404]\otimes\pi 9/2[404]$, $\nu 5/2[413]\otimes\pi 7/2[413]$, $\nu 3/2[422]\otimes\pi 5/2[422]$ and $\nu 1/2[431]\otimes\pi 3/2[431]$. As a continuation of the systematic studies of the beta-decay of even-even neutron-rich nuclei in the transitional region, the beta-decay of ^{110}Mo was studied in this work. This isotope is the most neutron-rich isotope of Mo whose decay has been observed up to now. Beta-decay of ^{110}Mo was observed for the first time at IGISOL a few years ago [10].

2 Experiment

The neutron-rich nucleus ^{110}Mo was produced by using 25 MeV proton-induced fission of ^{238}U. It was on-line mass separated from the other fission products using the ion guide technique. The proton beam with a typical intensity of 10 μA was delivered as 50 MeV H_2^+ ions by the

[a] *Present address*: Argonne National Laboratory, 9700 S. Cass Ave., Room F-133, Bldg 203, Argonne, IL 60439, USA; e-mail: jcwang@phy.anl.gov

Table 1. List of γ-rays from the decay of ^{110}Mo. 100 γ intensity units correspond to a β-feeding of 54%.

Energy (keV)	γ intensity	From	To	Coincident lines
39.4 (1)	< 8	39	0	(223)
53.3 (1)	19.8 (9)	53	0	132
121.0 (1)	41.3 (6)	263	142	142, 204, 273, 478
131.7 (1)	16.6 (5)	185	53	53
142.1 (1)	100	142	0	121, 204, 273, 326, 448, 478, 598, 767
203.6 (2)	2.0 (4)	467	263	121, 142, 223, 263, 273
223.4 (1)	21.1 (21)	263	39	(39), 204, 273, 478
262.9 (2)	8.2 (9)	263	0	204, 273, 478
273.0 (1)	2.9 (8)	741	467	121, 142, 204, 223, 263, 326
325.7 (1)	5.4 (3)	467	142	142, 273
447.6 (3)	2.3 (4)	590	142	142
477.8 (1)	25.6 (15)	741	263	53, 121, 132, 142, 223, 263
598.4 (1)	39.9 (20)	741	142	142
741.1 (2)	8.2 (10)	741	0	
766.7 (1)	6.5 (6)	909	142	142

$K = 130$ MeV cyclotron at the Accelerator Laboratory of the University of Jyväskylä. The uranium target was placed at an angle of 7° with respect to the beam direction in order to increase its effective thickness from 15 mg/cm^2 to 125 mg/cm^2. The ion guide method was based on thermalizing the primary recoil ions from the target as single charged ions in helium and guiding ions with helium flow and electric fields to a conventional mass separator [11]. The ion guide permits thermalized nuclear-reaction products to be injected directly into an isotope separator. Thus, the separation time and efficiency are independent of the volatility of the element. This technique is very efficient to investigate short half-life nuclei of refractory elements such as those between Zr and Rh. In principle, it can be used for radionuclei of all elements with half-lives even less than ms. Recent fission ion guide development and high proton beam intensity have substantially increased the yields of mass-separated ions [12]. At present, isobaric yields of the order of 10^5 ions/s are routinely available for medium-mass fission product beams [13]. The production rate of ^{110}Mo in this experiment was 42 atoms/s, which is 10 times higher than that of the previous experiment [10].

The mass-separated beams were implanted into a collection tape, which was moved at preset time intervals to reduce the β- and γ-background from longer-lived isobaric activities. Two 1 mm thick plastic scintillator detectors were placed on both sides of the implantation point for detection of β-particles. Laboratory and neutron-induced background were suppressed by measuring γ-rays in coincidence with β-decay. Three Ge detectors with relative efficiencies of 20%, 37% and 23%, respectively, were positioned in a plane around the collection spot at a distance of 30 mm and at angles of 90 degrees with respect to each other for the detection of γ-rays. The total efficiency for 1332 keV γ-rays was approximately 1.9%. The experimental data, including β-γ, β-γ-t and γ-γ coincidences, were recorded by means of the multiparameter data acquisition system VENLA and written on an exabyte tape for off-line analysis [14]. In the data analysis, a γ-TDC matrix was formed by summing all events from three Ge detectors in coincidence with β-particles as a function of the time of their occurrence within the measurement cycles. This matrix was used for half-life analysis. A γ-γ energy matrix was created off-line from all detector pairs by using a gain-matching algorithm from the EUROGAM software [15]. The γ-γ energy matrix was analyzed by using a set of programs on a VAX computer with general projection techniques to establish the decay scheme.

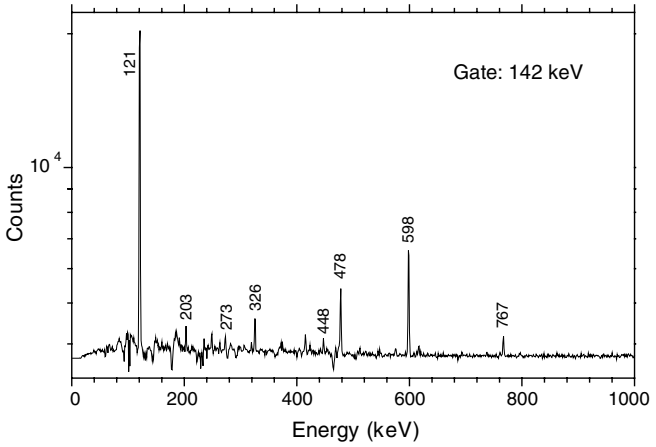

Fig. 1. γ-ray spectrum gated by the 142 keV transition of ^{110}Tc.

3 Results

The present experiment confirms the results of the previous study, which identified 6 excited states and 8 gamma transitions. In addition, we observe 3 new excited states and 7 new gamma transitions which can be attributed to the beta-decay of ^{110}Mo. Figure 1 displays the γ-ray spectrum gated by the 142 keV transition of ^{110}Tc. Transitions assigned to the β-decay of ^{110}Mo are listed in table 1. The relative γ-ray intensities were obtained from the β-gated singles γ-ray spectrum and the coincidence spectra. The

Table 2. Levels in ^{110}Tc fed in the decay of ^{110}Mo. Logft values are calculated with Q_β = 5.67 MeV [16] and $T_{1/2}$ = 0.27(1) s.

Energy (keV)	β-feeding (%)	log ft	I^π
0.0	0.0		(3^+)
39.4 (1)			
53.3 (1)	16.7 (7)	4.7	1^+
142.1 (1)	2.5 (12)	5.5	(1^+)
185.0 (1)	9.0 (4)	4.9	(1^+)
262.9 (1)	23.2 (13)	4.5	1^+
467.1 (2)	2.4 (5)	5.4	(1^+)
589.7 (1)	1.2 (2)	5.6	
740.8 (1)	41.4 (14)	4.1	1^+
908.8 (1)	3.5 (3)	5.1	(1^+)

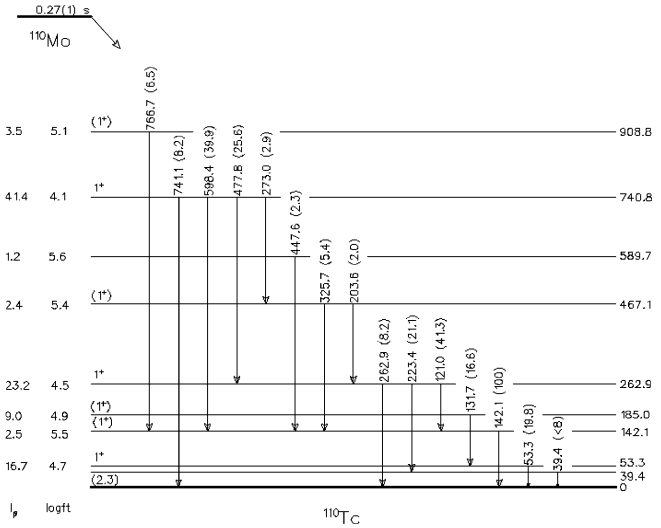

Fig. 2. Decay scheme of ^{110}Mo.

levels of ^{110}Tc fed in ^{110}Mo decay are listed in table 2 and the revised decay scheme is shown in fig. 2. The β-feedings and log ft values represent apparent values, *i.e.* assume that the decay scheme is complete.

A new γ transition of 263 keV was observed to connect the 263 keV level and the ground state.

A new level at 467 keV is introduced by observing new γ transitions at 204 and 326 keV in coincidence with the 121, 142 and 223 keV transitions and with the 142 keV transition, respectively.

A new 590 keV level is based on a new 448 keV γ transition in coincidence with 142 keV transition.

A new 273 keV transition was observed to connect the 741 keV level and the new level at 467 keV. It is in coincidence with the 121, 142, 223 and 326 keV transitions. A tentative transition from the 741 keV level to the ground state reported in [10] was confirmed by observing the 741 keV γ transition with the same half-life as the other γ lines of ^{110}Mo decay.

A new level at 909 keV is supported by a new 767 keV transition to the 142 keV level. The 767 keV transition is in coincidence with the 142 keV transition.

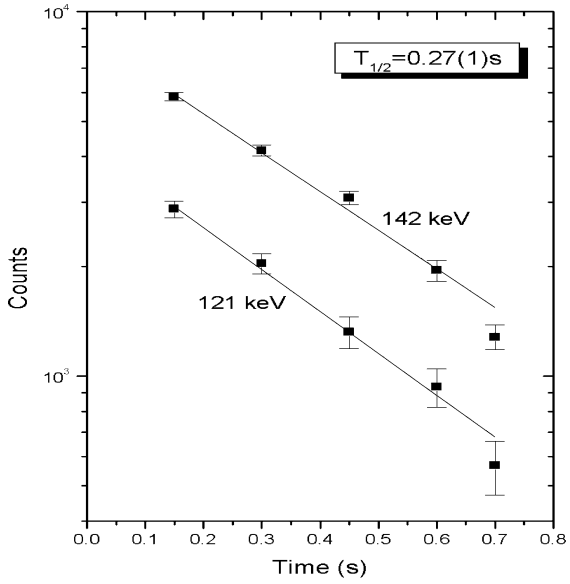

Fig. 3. Decay curves of the beta-gated 121 and 142 keV transitions in the decay of ^{110}Mo.

In the previous work the decay half-life of ^{110}Mo was determined as 0.30(4) s by fitting the decay curves of 142 keV γ-ray and the K_α X-rays [10]. Figure 3 displays the decay curves for the 121 keV and 142 keV γ transitions when gated by the beta detector. Half-lives obtained from these two decay curves as single component exponential fits are 0.26(1) s and 0.28(2) s, respectively.

Another decay study on ^{110}Tc suggests $I^\pi = 3^+$ for the ground state of ^{110}Tc [17]. Therefore, the β-feeding from ^{110}Mo to the ^{110}Tc ground state is negligible. The log ft values are calculated with Q_β = 5.67 MeV, deduced from the systematics [16]. This value is somehow higher than the decay energy of 4.9 MeV predicted by the finite-range droplet model [18]. The intensity of the 53 keV γ-ray was corrected for internal conversion on the basis of data measured in the previous work [10]. The systematic uncertainties caused by the internal conversion of the 121 and 132 keV transitions can be estimated to be less than 5% for β-branchings and 0.1 for log ft values. For the 142 keV level the β-feeding becomes 13% and the log ft value 4.8. The spin and parity of the excited states at 53, 263 and 741 keV are assigned to be 1^+ due to low log ft values of the feeding beta transitions. The excited states at 142, 185, 467 and 909 keV are relatively strongly fed in beta-decay suggesting a 1^+ character. Thus, this result implies that as many as 7 1^+ states are seen in the ^{110}Mo decay.

4 Discussion

A macroscopic-microscopic model described in [19] was applied to calculate the distribution of the GT strength in the beta-decay of ^{110}Mo. This model was successfully used to calculate the GT strength distribution for even-even $^{108-112}$Ru and $^{102-108}$Mo nuclei earlier [7,9]. The calculation is based on the deformed Woods-Saxon

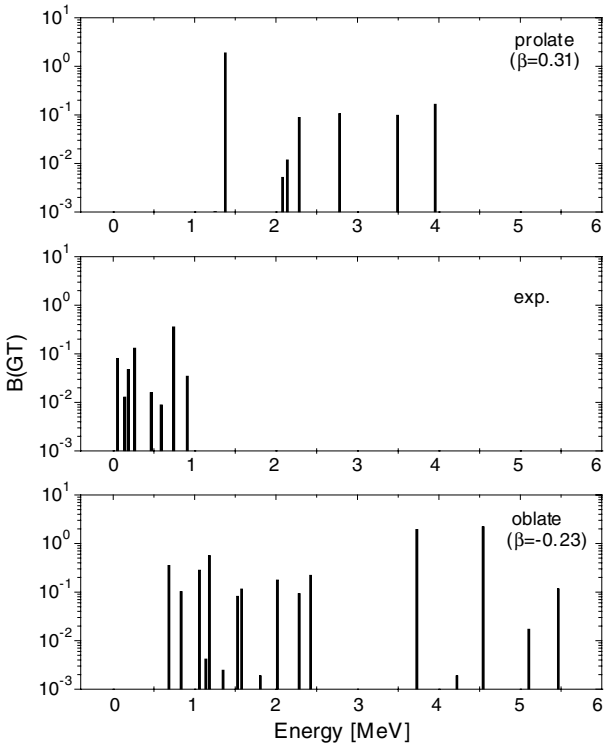

Fig. 4. Beta strength B(GT) distribution of ^{110}Mo over the calculated and experimental 1^+ states of ^{110}Tc. The calculated oblate and prolate states are presented in the bottom and top panels, respectively. Experimental states are presented in the middle panel.

potential using the shell correction method together with the liquid-drop formula of Myers and Swiatecki [20] and pairing treated in the Lipkin-Nogami extension of the BCS-approximation [21]. The calculation for each state was based on minimizing the nuclear potential energy as a function of the deformation parameters β_2 and β_4. Neutron states originating from the shell model states $d_{5/2}$, $g_{7/2}$, $s_{1/2}$, $d_{3/2}$ and $h_{11/2}$ and proton states from the $f_{5/2}$, $p_{3/2}$, $p_{1/2}$, $g_{9/2}$ and $d_{5/2}$ shell model states were included in the calculation of the two–quasi-particle states of the odd-odd daughter nuclei.

The calculation of the deformation of the ground state of ^{110}Mo shows two energy minima with almost identical energies, both well below the energy corresponding to the spherical shape. This implies that the ^{110}Mo nucleus is deformed in its ground state, but the sign of deformation remains unknown. The results calculated for both oblate and prolate states of ^{110}Mo are shown in fig. 4. The calculated 2–quasi-particle states of the daughter nucleus ^{110}Tc have a significant oblate or prolate deformation, except for the relatively high-lying spherical 1^+ state resulting from the coupling of the $9/2^+[404]$ neutron state and the $7/2^+[404]$ proton state. Due to large deformation of the parent nucleus, this state does not play an important role in the beta-decay pattern, because the decay from the deformed initial state to the spherical final state is "shape hindered". For the prolate deformation, the most important coupling among au transitions is $\nu 5/2^+[413]\otimes\pi 7/2^+[413]$. The energy of this state is at 1377 keV. The average energy of the prolate 1^+ states follows the energy of this state, due to its dominant role among the prolate final states. In the case of the oblate final states, the number of states is higher and there are two au transitions available, namely to the states with configuration $\nu 3/2^+[422]\otimes\pi 5/2^+[422]$ and $\nu 1/2^+[431]\otimes\pi 3/2^+[431]$. The calculated energies of these two states are at 1576 and 2017 keV.

Table 3. Beta-decay characteristics of ^{110}Mo compared with other neighbouring even Mo isotopes.

Isotope	$T_{1/2}$ (s)	Q_β (keV)	$\log ft$	B_Σ(GT)	E^*(ave)
^{102}Mo	678 (12)	1010 (23)	4.09	0.31	77
^{104}Mo	60 (2)	2155 (40)	4.13	0.29	382
^{106}Mo	8.73 (10)	3520 (17)	4.18	0.26	525
^{108}Mo	1.09 (2)	5120 (40)	4.14	0.28	396
^{110}Mo	0.27 (1)	5670	3.8	0.67	533

The experimental beta strength distribution is compared with theoretical calculation in fig. 4. In allowed β^--decay the reduced GT transition strength can be obtained by the formula $B(\mathrm{GT}) = 3864/ft$, where f is the phase space factor taken from [22] and t is the partial half-life in seconds and the constant 3864 s represents the constant $D = 6145$ s divided by the square of the free-nucleon value of the ratio of the axial to vector coupling constants $(g_\mathrm{A}/g_\mathrm{V}) = 1.263$ [23]. The total beta-decay strength is deduced by summing the strengths of the individual transitions through the relation $B_\Sigma(\mathrm{GT}) = 3864\Sigma(1/ft)$. Therefore, the total $\log ft$ value can be deduced. The experimental B(GT) distribution does not follow the trend of those calculated from either prolate states or oblate states. This might be due to the experimental sensitivity limited by more than three-orders stronger isobaric contamination. By the way, the information on the sign of deformation may be obtained by comparing the experimental average energy of the excited 1^+ states to the theoretical average energies of prolate states and oblate states. The average energy of the excited 1^+ states is calculated according to the relation $E^*(\mathrm{ave}) = (\Sigma_i B_i E_i^*)/(\Sigma_i B_i) \approx \bar{E}(1^+)$. The average energy of prolate states is 1.8 MeV, while that of oblate states is 3.4 MeV. Both of them are far away from the experimental average energy of the excited 1^+ states, which is 533 keV. However, comparing with the value of oblate states, the average energy of prolate states is much closer to the experimental value. This might be an indication of prolate deformation for ^{110}Mo. The beta-decay gross properties of ^{110}Mo are summarized in table 3 including those of $^{102-108}$Mo for comparison [9]. The experimental average energy of the excited 1^+ states of $^{104-110}$Mo keeps nearly constant, while the model predicts the average energies of 1^+ states increase with respect to increasing neutron number [9].

5 Conclusion

Reinvestigation of the beta-decay of ^{110}Mo leads to some new results. Comparison between the experimental

data and the theoretical calculation of a macroscopic-microscopic model does not show a clear evidence for the shape of ^{110}Mo. It remains an open question. Recent development of a Penning trap system on the IGISOL facility for purification of isobaric contamination will improve sensitivity and precision of the experiments extremely. This will make the level lifetime measurement of ^{110}Mo possible. Therefore, the problem of the interpretation of the shape of ^{110}Mo can be finally solved.

This experiment has been financially supported by the Academy of Finland and by the access to the Large Scale Facilities programme under the TMR programme of the European Union. This work is part of a PhD work (J.C. Wang).

References

1. S.G. Nilsson, Dan. Mat. Fys. Medd. **29**, no. 16 (1955).
2. G. Alaga, Phys. Rev. **100**, 432 (1955).
3. J.-I. Fujita, G.T. Emery, Phys. Rev. C **1**, 2060 (1970).
4. P.C. Sood, At. Data Nucl. Data Tables **43**, 259 (1989).
5. V. Koponen, J. Äystö, J. Honkanen, P.P. Jauho, H. Penttilä, J. Suhonen, P. Taskinen, K. Rykaczewski, J. Zylicz, C.N. Davids, Z. Phys. A **333**, 339 (1989).
6. Z. Janas, J. Äystö, K. Eskola, P.P. Jauho, A. Jokinen, J. Kownacki, M. Leino, J.M. Parmonen, H. Penttilä, J. Szerypo, J. Zylicz, Nucl. Phys. A **552**, 340 (1993).
7. A. Jokinen, J. Äystö, P. Dendooven, K. Eskola, Z. Janas, P.P. Jauho, M. Leino, J.M. Parmonen, H. Penttilä, K. Rykaczewski, P. Taskinen, Z. Phys. A **340**, 21 (1991).
8. A. Jokinen, J. Äystö, P.P. Jauho, M. Leino, J.M. Parmonen, H. Penttilä, K. Eskola, Z. Janas, Nucl. Phys. A **549**, 420 (1992).
9. A. Jokinen, T. Enqvist, P.P. Jauho, M. Leino, J.M. Parmonen, H. Penttilä, J. Äystö, K. Eskola, Nucl. Phys. A **584**, 489 (1995).
10. G. Lhersonneau, A. Honkanen, M. Huhta, P.P. Jauho, A. Jokinen, M. Leino, M. Oinonen, E. Ollikainen, J.M. Parmonen, J. Äystö, Z. Phys. A **350**, 97 (1994).
11. P. Dendooven, Nucl. Instrum. Methods B **126**, 182 (1997).
12. H. Penttilä, P. Dendooven, A. Honkanen, M. Huhta, G. Lhersonneau, M. Oinonen, J.M. Parmonen, K. Peräjärvi, J. Äystö, Nucl. Instrum. Methods B **126**, 213 (1997).
13. M. Huhta, P. Dendooven, A. Honkanen, G. Lhersonneau, M. Oinonen, H. Penttilä, K. Peräjärvi, V. Rubchenya, J. Äystö, Nucl. Instrum. Methods B **126**, 201 (1997).
14. K. Jääskeläinen, P.M. Jones, A. Lampinen, K. Loberg, W. Trzaska, JYFL Annual Report (1995) p. 15.
15. J. McPherson, IEEE Trans. Nucl. Sci. **39**, 806 (1992).
16. G. Audi, W.H. Wapstra, Nucl. Phys. A **565**, 1 (1993).
17. J.C. Wang, G. Canchel, P. Dendooven, J.H. Hamilton, S. Hankonen, J. Huikari, J.K. Hwang, A. Jokinen, V.S. Kolhinen, G. Lhersonneau, A. Nieminen, V.E. Oberacker, K. Peräjärvi, A.V. Ramaya, J. Äystö, Phys. Rev. C **61**, 044308 (2000).
18. P. Möller, J.R. Nix, K.-L. Kratz, At. Data Nucl. Data Tables **66**, 131 (1997).
19. J. Dobaczewski, W. Nazarewicz, A. Plochocki, K. Rykaczewski, J. Zylicz, Z. Phys. A **329**, 267 (1988).
20. W.D. Myers, W. Swiatecki, Nucl. Phys. **81**, 1 (1966); Ark. Fys. **36**, 343 (1967).
21. H.C. Pradham, Y. Nogami, J. Law, Nucl. Phys. A **201**, 357 (1973).
22. N.B. Gove, M.J. Martin, At. Data Nucl. Data Tables **10**, 205 (1971).
23. I.S. Towner, Nucl. Phys. A **444**, 402 (1985).